Discovery Process and Pharmacological Characterization of 2-(*S*)-(4-Fluoro-2-methylphenyl)piperazine-1-carboxylic Acid [1-(*R*)-(3,5-Bis-trifluoromethylphenyl)ethyl]methylamide (Vestipitant) as a Potent, Selective, and Orally Active NK_1 Receptor Antagonist

Romano Di Fabio,*[,#] Cristiana Griffante,[#] Giuseppe Alvaro,[#] Giorgio Pentassuglia,[#,†] Domenica A. Pizzi,[#] Daniele Donati,[#,§] Tino Rossi,[#] Giuseppe Guercio,[‡] Mario Mattioli,[‡] Zadeo Cimarosti,[‡] Carla Marchioro,[||] Stefano Provera,[||] Laura Zonzini,[#] Dino Montanari,[#] Sergio Melotto,[#] Philip A. Gerrard,[#] David G. Trist,[#] Emiliangelo Ratti,[#] and Mauro Corsi[#]

Neurosciences Centre of Excellence for Drug Discovery, Chemical Development, and Molecular Discovery Research, GlaxoSmithKline Medicines Research Centre, Via A. Fleming 4, 37135 Verona, Italy

Received January 9, 2009

In an effort to discover novel druglike NK_1 receptor antagonists a new series of suitably substituted *C*-phenylpiperazine derivatives was identified by an appropriate chemical exploration of related *N*-phenylpiperazine analogues, with the specific aim to maximize their in vitro affinity and optimize in parallel their pharmacokinetic profile. Among the compounds synthesized, 2-(*S*)-(4-fluoro-2-methylphenyl)piperazine-1-carboxylic acid [1-(*R*)-(3,5-bis-trifluoromethylphenyl)ethyl]methylamide (vestipitant) was identified as one of the most in vitro potent and selective NK_1 receptor antagonists ever discovered, showing appropriate pharmacokinetic properties and in vivo activity. On the basis of its preclinical profile, this compound was selected as a drug candidate.

Introduction

A large body of preclinical and clinical evidence associate the substance P (SP[a]) and its preferred G-protein-coupled receptor (GPCR) NK_1 with the pathophysiology of a variety of stress and fear-related disorders,[1−5] including depression, a pathological condition still perceived as one of the leading disabling illnesses worldwide.[6,7] In addition, since SP is widely spread within the CNS and colocalized with relevant neurotransmitters, it has been hypothesized to be critical to the control of nociception, migraine, nausea and vomiting, inflammatory bowel syndrome, and urinary incontinence.[8,9] From the past 15 years to date, this large therapeutic potential triggered an unprecedented industrial research effort aimed toward the discovery and the clinical evaluation of NK_1 receptor antagonists. In phase II clinical trials performed by Merck and Pfizer, MK-869,[10] L-759274,[11] and CP-122,721[12] (Figure 1) have proven to be antidepressants. In addition, Novartis reported for NKP-608[13] (Figure 1) positive result in a clinical trial in patients with social phobia, whereas GSK showed that GR205171 (Figure 1) was able to reduce significantly anxiety symptoms involving 36 patients suffering from social anxiety disorders (SAD).[14] Finally MK-869 (Emend) has been launched into the market as an antiemetic agent for chemotherapy-induced nausea and both acute and delayed vomiting (CINV). Notably, all of the NK_1 receptor antagonists tested in humans so far seem to be well tolerated with a cleaner side effects profile with respect to classical antidepressant agents (SSRIs, SNRIs, and tricyclics).[10,11,15,16]

As part of a wide drug discovery program aimed toward the identification of a novel series of NK_1 receptor antagonists, phenylpiperazine derivatives of type A, shown in Figure 2, were designed both to maximize the recognition of the NK_1 receptor binding site and to maintain the positive physicochemical features associated with GR205171,[17] one of the most druglike compounds identified at that time. Herein we describe the exploration and the structure−activity relationship (SAR) of this new class of NK_1 receptor antagonists. The screening cascade set up to select the best compounds included in vitro studies at recombinant human NK_1 receptors and an in vivo pharmacodynamic model in gerbil, a species that has shown a similar NK_1 receptor pharmacology as the human NK_1 receptor.[18,19] Among the compounds identified, **14aa** was found to be a potent, selective, and orally active NK_1 receptor antagonist.[20]

Chemistry

The racemic derivative **7** was prepared as shown in Scheme 1. Intermediate **4** was synthesized in two steps from **2** and in high chemical yield by sequential Suzuki-type cross coupling reaction and followed by hydrogenation of the pyrazine ring. Then the chemoselective protection of the less hindered nitrogen atom as Cbz afforded key intermediate **5**. The following coupling reaction was performed with triphosgene and triethylamine followed by addition of *N*-methyl-3,5-bis(trifluoromethyl)benzylamine hydrochloride in CH_2Cl_2 at 0 °C in the presence of pyridine to give intermediate compound **6**, which was then transformed into the racemate **7** by hydrogenation. The synthesis of the pure enantiomers **7a** and **7b** was performed as shown in Scheme 2. Compound **4** was transformed into the diastereomeric mixture **8a**,**b** in the presence of CDI and (*R*)-(+)-1-phenethyl alcohol. The following elaboration of the right-hand side of the molecule enabled us to prepare diastereoisomers **9a** and **9b**, which were separated by flash chromatography.

* To whom correspondence should be addressed. Phone: +39 045 8218879. Fax: +39 045 8218196. E-mail: rdf26781@gsk.com.

[#] Neurosciences Centre of Excellence for Drug Discovery.

[†] Present address: E-Pharma Trento S.p.A., Via Provina 2, 38040 Ravina di Trento, Trento, Italy.

[§] Present address: Nerviano Medical Sciences Srl, Via Pasteur 10, 20014 Nerviano, Milan, Italy.

[‡] Chemical Development.

[||] Molecular Discovery Research.

[a] Abbreviations: NK, neurokinin; SP, substance P; GPCR, G-protein-coupled receptor; CNS, central nervous system; SAD, social anxiety disorders; CINV, chemotherapy-induced nausea and vomiting; SSRIs, selective serotonin reuptake inhibitors; SNRIs, selective norepinephrine reuptake inhibitors; SAR, structure−activity relationship; CDI, carbonyldiimidazole; THF, tetrahydrofuran; CHO, Chinese hamster ovary; FLIPR, fluorescence imaging plate reader; GFT, gerbil foot tapping; CRC, concentration−response curve.

10.1021/jm900023b CCC: $40.75
Published on Web 04/23/2009

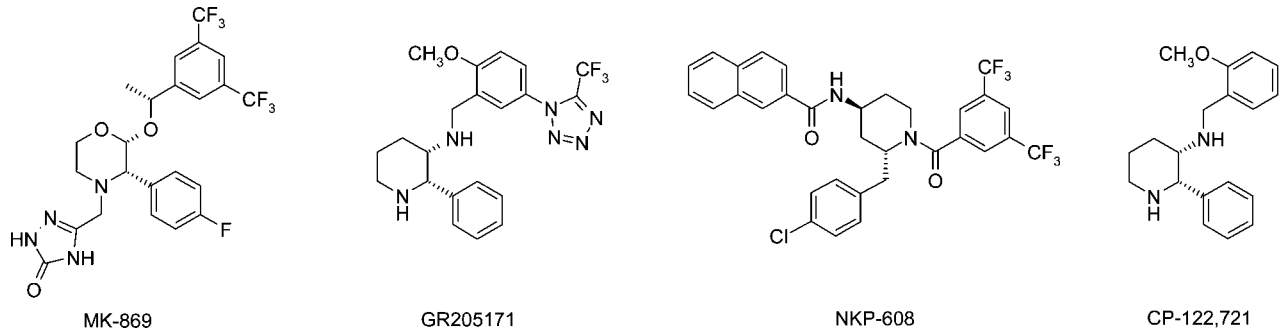

Figure 1. Chemical structures of some NK1 receptor antagonists evaluated in clinical trials.

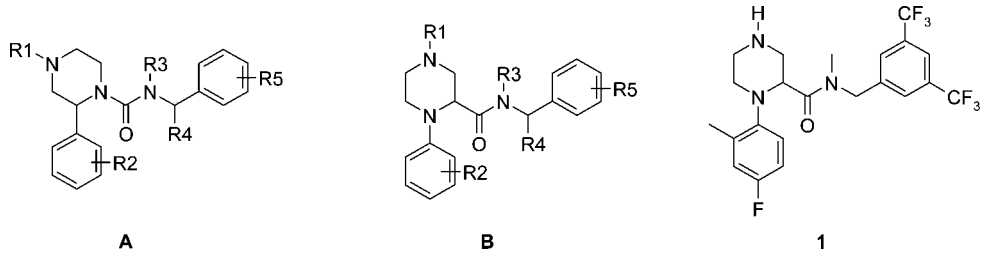

Figure 2. General structures of the *C*-phenylpiperazines and *N*-phenylpiperazines.

Scheme 1[a]

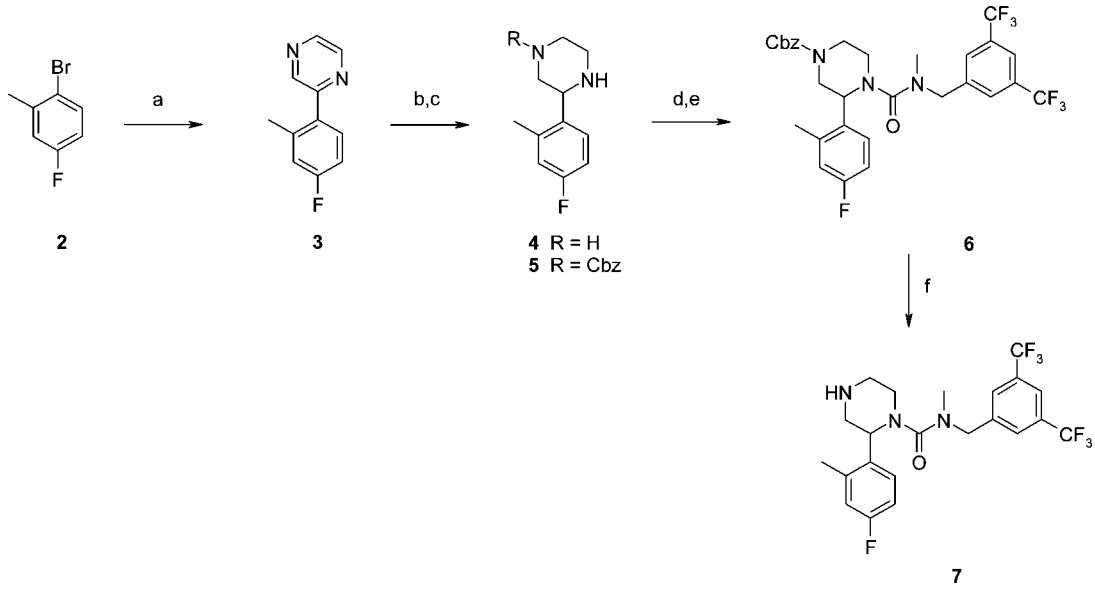

[a] (a) [1,2-Bis(diphenylphosphino)-ethane]dichloronickel (II), chloropyrazine, Na_2CO_3 1 M, toluene, EtOH 95%, 2 h, reflux; (b) 20% $Pd(OH)_2/C$, H_2 (5 atm), 95% EtOH/37% HCl, 100:1, 4 h; (d) benzylchloroformate, Et_3N, CH_2Cl_2, $T = 0$ °C, 2 h; (e) triphosgene, Et_3N, CH_2Cl_2, $T = 0$ °C, 3 h, then *N*-methyl-3,5-bis(trifluoromethyl)benzylamine hydrochloride, pyridine, CH_2Cl_2, room temp, 12 h.; (f) (i) H_2 (1 atm), 10% Pd/C, EtOH, 3 h; (ii) 1 M HCl/Et_2O.

Finally, the removal of the carbamate protecting group by hydrogenation reaction in the presence of 10% Pd/C afforded the title enantiomers **7a** and **7b**.

Single diasteroisomers **14aa**, **14ab**, **14ba**, and **14bb** were synthesized as shown in Scheme 3. The Grignard reagent obtained from commercially available 2-bromo-5-fluorotoluene **2** was added to LiBr and Cu_2Br_2 in anhydrous THF and then reacted with methyloxalyl chloride to give intermediate **10**. The following reaction with ethylenediamine afforded the cyclized compound **11** in good yield, which was smoothly transformed into the key ketopiperazine **12** by hydrogenation in the presence of 10% Pd/C. The resolution of this racemate into the pure enantiomers **12a** and **12b** was achieved by crystallization of the corresponding *S*-(+)-mandelic acid and *R*-(−)-mandelic acid salt, respectively, in AcOEt. Then the two mixtures of diasteroisomers **13aa** and **13ab** were prepared from **12a** by reaction with triphosgene in CH_2Cl_2 at 0 °C in the presence of triethylamine, followed by addition of racemic 1-[3,5-bis(trifluoromethyl)phenyl]ethyl]-*N*-methylamine. The final separation by flash chromatography enabled us to get pure **13aa** and **13ab**, which were then reduced in the presence of $BH_3 \cdot THF$ in THF to give title compounds **14aa** and **14ab**. Then single diastereoisomers **14ba** and **14bb** were prepared from **12b** following the same synthetic procedure.

Results and Discussion

To identify an innovative series of NK_1 receptor antagonists, our chemical strategy was initially focused on the exploration of the *N*-phenylpiperazines of type B, compounds discovered by an internal screening (Figure 2). In particular, compound **1**

Scheme 2[a]

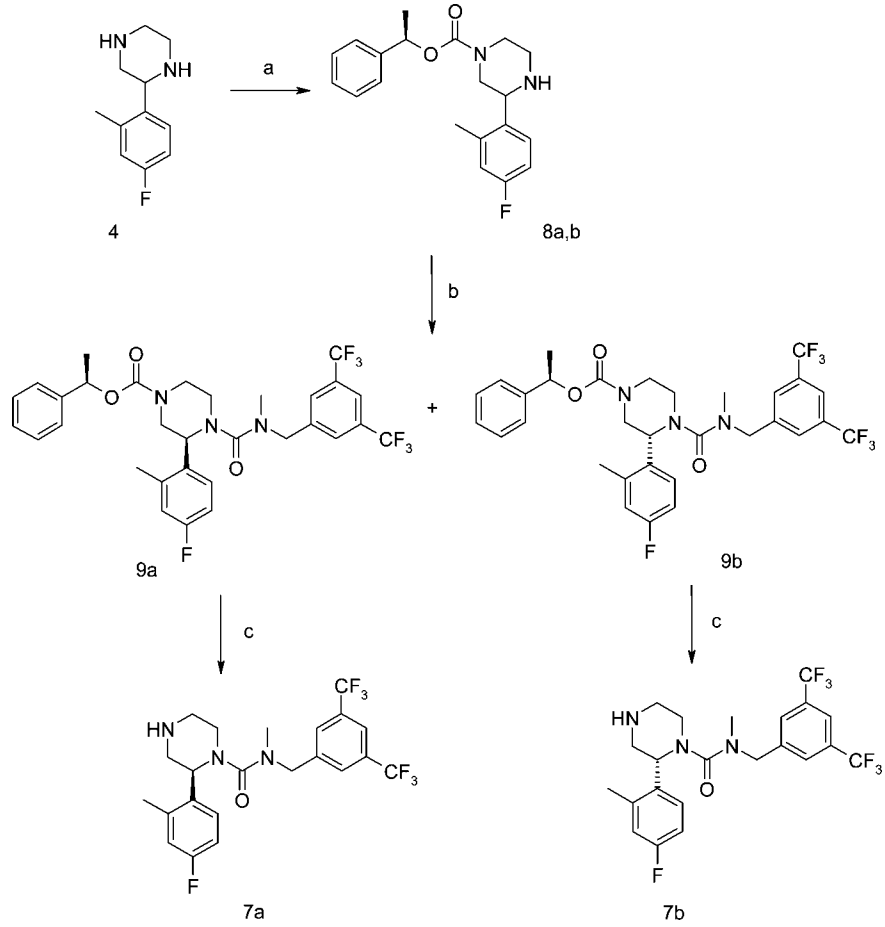

[a] (a) CDI, (*R*)-(+)-1-phenylethyl alcohol, CH_2Cl_2, 30 min, room temp, then **4**, CH_3CN, reflux, 24 h; (b) triphosgene, Et_3N, CH_2Cl_2, $T = 0$ °C, 2 h, then *N*-methyl-bis-3,5-(trifluoromethyl)benzylamine hydrochloride, 4 h, room temp; (c) (i) H_2 (1 atm), 10% Pd/C, 95% EtOH, 4 h; (ii) 1 M HCl/Et_2O.

Table 1. In Vitro Binding Affinities (pK_i)/Functional Potencies (pK_B) at h-NK_1 Receptors and in Vivo Activity of NK_1 Receptor Antagonists in the Gerbil Foot Tapping Model (GFT)

compd	pK_i (pK_B)[a]	*n*	ID_{50}, mg/kg[b]
GR205171	10.30 ± 0.08	5	0.6
1	8.06 ± 0.07 (8.56 ± 0.02)	5 (3)	NT[c]
7	8.89 ± 0.05	8	NT[c]
7a	9.37 ± 0.07	8	0.2
7b	7.74 ± 0.15	3	5.6
14aa	9.65 ± 0.14 (9.87 ± 0.06)	5 (3)	0.014
14ab	9.27 ± 0.04	3	0.036
14ba	8.09 ± 0.12	6	NT[c]
14bb	8.43 ± 0.06	3	NT[c]

[a] pK_i and pK_B values have been determined as described in Experimental Section and are the mean ± SEM of *n* experiments performed in duplicate. [b] ID_{50} is the compound dose causing 50% inhibition of the tapping behavior elicited by the icv injection of GR73632, 3 pmol/5 μL. ID_{50} values are expressed in mg/kg after oral or subcutaneous administration 1 h before the test. [c] NT = not tested.

exhibited promising in vitro potency ($pK_i = 8.06$; Table 1), measured by inhibition of the binding of [^{3}H]substance P ([^{3}H]SP) to membranes obtained from Chinese hamster ovary cells transfected with human NK_1 receptors (h-NK_1 CHO). The antagonist profile of compound **1** was then investigated in fluorescence imaging plate reader (FLIPR) functional studies where it was shown to antagonize in a competitive manner SP-induced $[Ca^{2+}]_i$ in h-NK_1 CHO cells with a pK_B value of 8.56 (Table 1, Figure 4A). To maximize the in vitro affinity of this molecule, we proposed to modify the *N*-phenylpiperazine core into the *C*-phenylpiperazine template of type A, shown in Figure 2. This structural modification, if tolerated, would have enabled us to identify compounds with improved druggability, in terms of limited molecular weight with respect to the known NK_1 receptor antagonists series and appropriate basicity of the nitrogen atom. Following this novel structural hypothesis, compound **7** was prepared as a racemate and characterized in terms of in vitro affinity at the NK_1 receptor binding site. As shown in Table 1, a significant improvement was observed with respect to the corresponding *N*-phenylpiperazine derivative **1** (pK_i of 8.89 and 8.06 for compounds **7** and **1**, respectively), confirming the possibility of getting higher in vitro affinity depending upon a more accurate positioning of the nitrogen atoms within the phenylpiperazine template. Notably, as shown in Table 1, the two enantiomers **7a** and **7b**, prepared as reported above, exhibited significant differences in terms of in vitro affinity ($pK_i = 9.37$ and $pK_i = 7.74$, respectively), being that (*S*)-enantiomer **7a** is the most active. Further to this result, **7a** was then tested in the gerbil foot tapping (GFT) model. This model represents a pharmacodynamic test to assess central NK_1 receptor antagonism. Indeed, brain penetrant compounds when administered systemically were able to inhibit the tapping behavior elicited by intracerebroventricular (icv) injection of 3 pmol (5 μL) of the NK_1 receptor agonist GR73632 (see Experimental Section). As shown in Table 1, an excellent in vivo activity was observed with **7a** after oral and subcutaneous administration ($ID_{50} = 0.2$ mg/kg, both routes of administration). Notably, a long lasting effect was observed because that compound was still active 8 h after its oral administration (ID_{50}

Scheme 3[a]

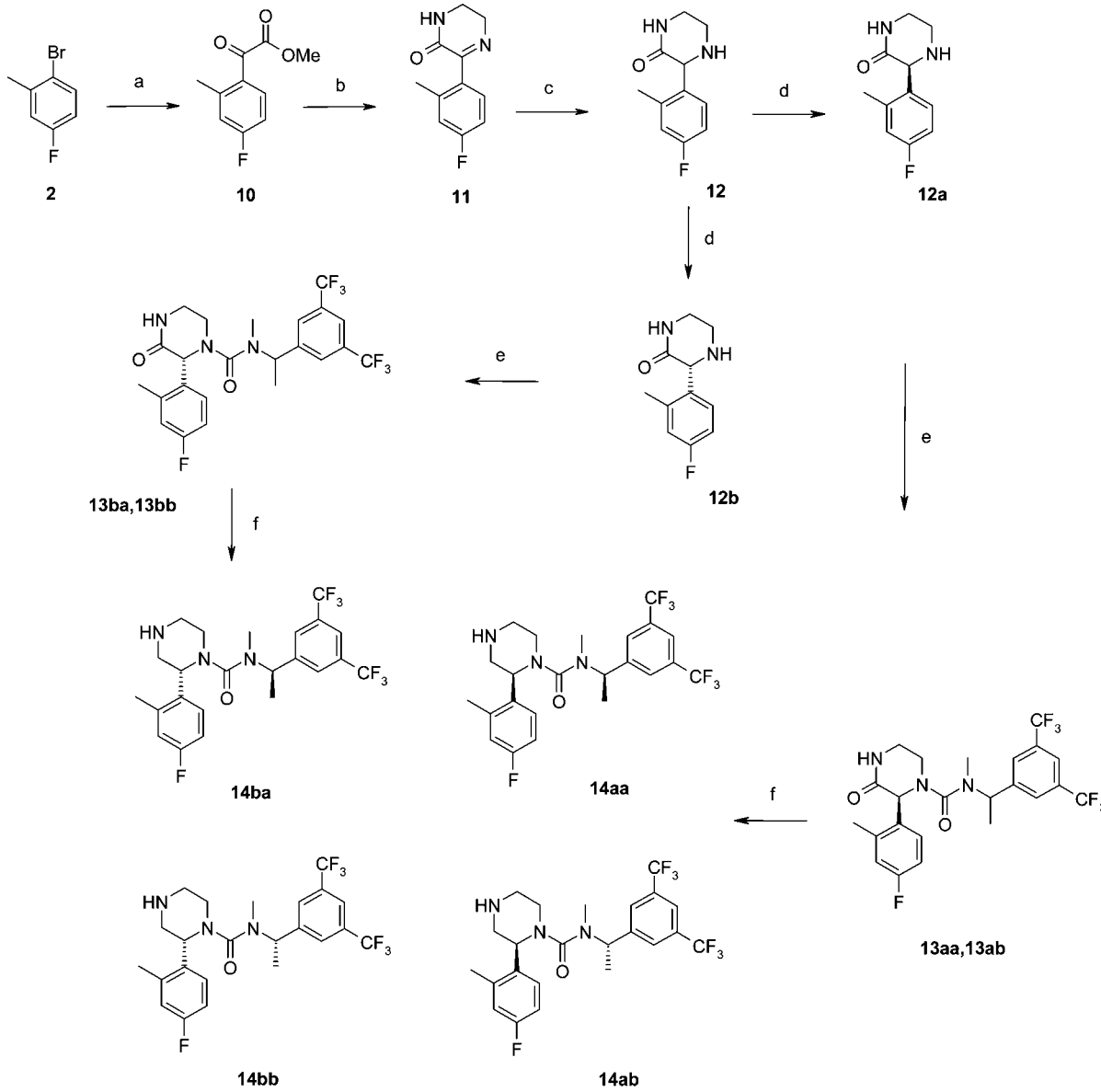

[a] (a) (i) Mg, I_2, THF, $T = 70$ °C, 2 h; (ii) LiBr, Cu_2Br_2, THF, room temp 1 h; (iii) $CH_3OCOCOCl$, room temp, 2 h; (b) ethylenediamine, toluene, reflux, 6 h; (c) H_2 (1 atm), 10% Pd/C, MeOH, 16 h; (d) (i) *S*-(+)-mandelic acid or *R*-(−)-mandelic acid, AcOEt, $T = 3-5$ °C, 2 h; (ii) filtration of the salt, then crystallization in AcOEt; (iii) 0.73 M NaOH; (e) (i) triphosgene, Et_3N, CH_2Cl_2, $T = 0$ °C, 4 h; (ii) 1-[3,5-bis(trifluoromethyl)phenyl]ethyl]-*N*-methylamine, $N(i\text{-}Pr)_2Et$, CH_3CN, $T = 70$ °C, 2 h; (f) (i) 1 M BH_3·THF, THF, reflux, 3 h; (ii) Et_2O, AcOH.

= 0.3 mg/kg), suggesting that **7a** was still present in the brain after several hours from its administration.

Further to the identification of compound **7a**, the effect of the substitution of the benzylic position by a methyl group was explored. To this end the single diastereoisomers **14aa**, **14ab**, **14ba**, and **14bb** were synthesized. Their in vitro affinities at h-NK_1 receptors are shown in Table 1. As expected, among them, **14aa** and **14ab** were the most potent ones, suggesting once again the importance of the correct stereochemistry of the stereogenic center present in the phenylpiperazine core (Figure 3). Conversely, the in vitro affinities of **14aa** and **14ab** are only slightly different, making the stereochemistry of the benzylic position less critical.

Oral administration of **14aa** (0.01−0.1 mg/kg), prior to icv infusion of GR73632, caused a dose dependent and complete inhibition of foot tapping in gerbils with an estimated ID_{50} of 0.014 mg/kg (Table 1), suggesting a potent central activity of the compound. Moreover, a time course study showed that the potency of **14aa** increased between 1 and 4 h (ID_{50} from 0.014 to 0.002 mg/kg); notably, 8 h after administration of the compounds, the effect was still present (Table 2).

Compound **14ab** was also tested in the GFT model, and in agreement with its reduced binding potency, it was found to be slightly less active ($ID_{50} = 0.036$ mg/kg, po) than **14aa** (Table 1).

Considering the greater in vitro and in vivo potency observed for **14aa**, an extensive pharmacological characterization of this compound was conducted. In particular, when this compound was preincubated for 60 min at 37 °C (3, 5, and 10 nM), it antagonized SP-induced $[Ca^{2+}]_i$ increase in h-NK_1 CHO cells. The type of antagonism observed was nonsurmountable (Figure 4B), since it was characterized by a rightward shift of the SP concentration−response curve (CRC) with a concentration-dependent reduction of the agonist maximal response. The apparent pK_B estimated at 3 nM concentration was 9.87 (Table 1). The nonsurmountable antagonism observed in in vitro studies

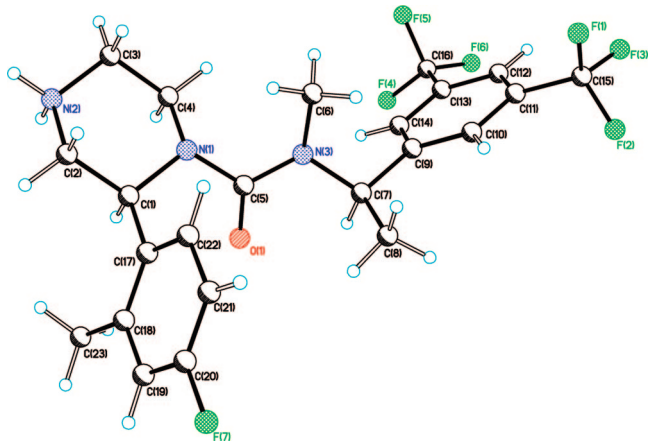

Figure 3. X-ray structure of compound **14aa**.

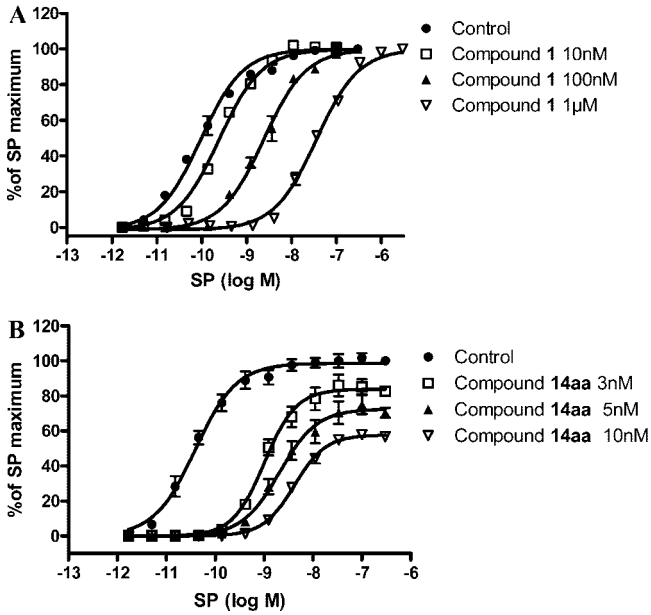

Figure 4. Antagonism of SP-induced increase of cytosolic calcium in h-NK_1 CHO cells by compound **1** (A) and compound **14aa** (B) in h-NK_1 CHO cells. Curves depicted are the mean fit of three independent experiments performed in duplicate.

Table 2. Effect of 1**4aa** on Gerbil Foot Tapping Test at Different Times (h) of Oral Pretreatment[a]

14aa	−1 h	−2 h	−4 h	−8 h
ID_{50} (mg/kg, po)	0.014	0.007	0.002	0.027
lower 95% CI	0.007	0.001	0.0009	0.020
upper 95% CI	0.020	0.014	0.009	0.035

[a] Data are presented as ID_{50} values (compound dose causing 50% inhibition of the tapping behavior elicited by the icv injection of GR73632, 3 pmol/5 μL).

by **14aa** could potentially indicate a noncompetitive behavior of the compound interacting with nonspecific sites of the h-NK1 receptor or with the coupling systems. To rule out these possibilities, the following in vitro studies using the combined dose ratio analysis[21] and the radioactive form of **14aa** were carried out. In particular, the competitive or noncompetitive nature of antagonism elicited by **14aa** with respect to the known competitive antagonist L-733,060[22] was investigated. As shown in Figure 5, the cumulative effect of 10 nM **14aa** and 100 nM L-733,060 rightward-shifted the agonist CRC in an additive model, rather than a multiplicative model, revealing a syntopic effect of the two antagonists in inhibiting SP response. Moreover, L-733,060 partially antagonized **14aa**-induced depression of the SP maximal response, in agreement with the syntopic action elicited by **14aa**. Saturation binding analysis in membranes from h-NK_1 CHO cells with increasing concentrations of [^{3}H]**14aa** indicated the presence of a single high affinity binding site, with a dissociation constant of 0.030 nM (pK_d = 10.52) (Figure 6). Kinetic binding studies of [^{3}H]**14aa** in membranes from h-NK_1 CHO cells revealed that the rate constant for the association of 0.2 nM radioligand with the h-NK_1 receptor is 0.0988 min^{-1} with a $t_{1/2}$ of 7.01 min and a $t_{99/100}$ of 46.6 min at 37 °C (Figure 7A). [^{3}H]**14aa** dissociated from the h-NK_1 receptor with simple monophasic kinetics with a rate of dissociation (k_{-1}) of 0.0116 min^{-1} and $t_{1/2}$ for receptor occupancy of 59.7 min (Figure 7B). Calculation of the K_D from the ratio of the kinetic parameters k_{off}/k_{on} gave a value of 0.027 nM (pK_D = 10.57). Taking together the kinetic binding and the functional data, it is suggested that the nonsurmountable effect of **14aa** versus SP is due to its long dissociation time from the NK_1 receptor, thus revealing a pseudoirreversible phenomenon of the compound rather than a noncompetitive action.

The receptogram screen (by MDS Pharma Service, Taiwan) confirmed that **14aa** is highly selective for the h-NK_1 receptor, since at 1 μM concentration it produced less than 50% displacement of binding in the full battery of 83 receptors, transporters, ion channels, and enzymes.

Compound **14aa** also exhibited excellent pharmacokinetics in vivo, both in rat and in dog (F = 44% and 71%, respectively) with a limited clearance in plasma (Cl_p = 19 and 15 (mL/min)/kg, respectively) and suitable half-life (5 and 11 h, respectively). As far as the brain penetration in rats is concerned, a B/P ratio of 1.3 was assessed 5 min after the intravenous administration of the compound at 1 mg/kg dose.

Conclusion

In conclusion an appropriate optimization strategy of the *N*-phenylpiperazine series available in house enabled us to identify a new class of potent and selective NK_1 receptor antagonist exhibiting remarkable druglike properties. In particular, compound **14aa** represents one of the most potent in vitro and in vivo NK_1 receptor antagonist ever identified. In particular, when administered orally to gerbil, **14aa** was found to inhibit the animal's foot tapping with long lasting pharmacological activity, exhibiting both an excellent pharmacokinetics profile and peculiar receptor kinetic behavior, namely, a slow dissociating rate of the ligand from the NK_1 receptor. This behavior was further supported by the nonsurmountable receptor interaction observed in vitro. In this respect, simulation studies demonstrated that a prolonged in vivo receptor occupancy should take place when the antagonist receptor complex dissociates more slowly than the antagonist gets eliminated.[23] This implies that the in vivo duration of action of an antagonist should depend not only on its rate of elimination via excretion and/or metabolism but also on the rate it dissociates from the receptor. Hence, slowly dissociating NK1 receptor antagonists may exert a substantially longer therapeutic action than the corresponding surmountable antagonists, a characteristic that is fundamental to drug discovery strategy to select the best possible clinical candidates.

Experimental Section

All the NMR spectra were recorded in DMSO-d_6 or $CDCl_3$ at a constant temperature of 25 °C, and complete assignments were made by means of several 1D and 2D techniques including ^{19}F, gCOSY, gHSQC, and gHMQC NMR experiments when needed.

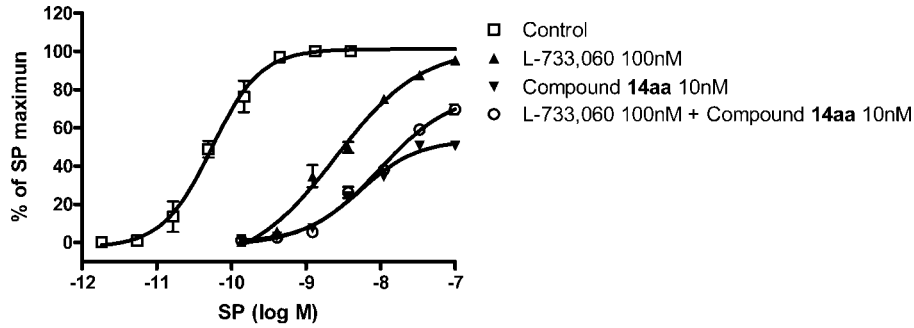

	Observed DR	Expected DR
14aa (10nM)	92	
L-733,060 (100 nM)	55	
14aa + L-733,060	172	
Multiplicative model (**14aa** + L-733,060)		5047
Additive model (**14aa** + L-733,060)		146

Figure 5. Antagonism of SP-induced increase of cytosolic calcium in h-NK_1 CHO cells. Combined dose ratio (DR) analysis between **14aa** and L-733,060 demonstrated that **14aa** acts competitively with respect to L-733,060. The observed DR of the combination study was found to be closer to the additive rather than to the multiplicative model (syntopic action).

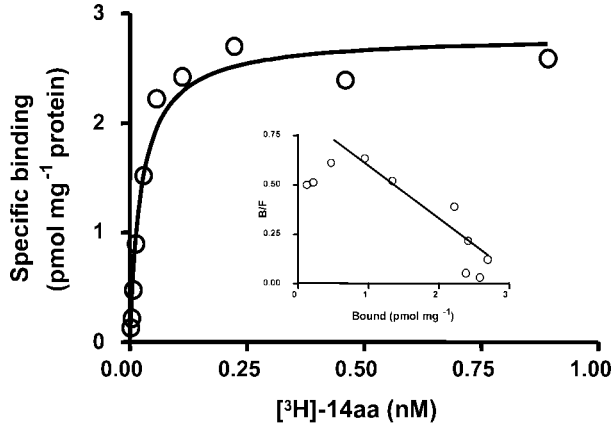

Figure 6. Representative [^{3}H]**14aa** saturation curve in membranes from CHO cells stably transfected with h-NK_1 receptor. Inset is the Scatchard plot.

^{1}H and gHSQC experiments were collected on a 400 Unity Varian or 500 Inova Varian instrument, and ^{13}C and ^{19}F experiments were collected using a 300 Inova Varian instrument. Chemical shifts are reported in parts per million (ppm) downfield from the $CHCl_3$ residual line (δ = 7.27 ppm) or from DMSO residual line (δ = 2.49 ppm) and were assigned as singlets (s), doublets (d), triplets (t), quartet (q), broad quartet (bq), broad singlets (bs), doublets of doublets (dd), or multiplets (m). Coupling constants (*J*) are given in Hz. IR spectra were recorded on a Nicolet Magna 760 (Thermo Fisher Scientific) spectrometer. Mass spectra analyses were performed on a VG Platform (Waters, Manchester, U.K.), with the mass spectrometer operating in positive electrospray ion mode. Analytical thin layer chromatography (TLC) was performed on glass plates (Merck Kieselgel 60 F254). Visualization was accomplished by UV light (254 nm), I2. Column chromatography was performed on silica gel (Merck Kieselgel 70−230 mesh). Melting points (mp) are uncorrected. Optical rotation $[\alpha]_D$ values were obtained in solution at the sodium D line at 20 °C. Chemical purity of compounds has been assessed by HPLC (>95%). For chiral HPLC analysis, condition A was as follows: purity of intermediates **12a** and **12b** was assessed using a Chiralcel OJ (4.6 mm × 250 mm) column from Daicel using *n*-hexane/ethanol, 80:20 v/v, as mobile phase (flow of 1 mL/min, UV detector at 265 nm, injection of 5 μL). Condition B was as follows: purity of compounds **14aa**, **14ab**, **14ba**, and **14bb** was assessed using a Chiralpack AD column (4.6 mm × 250 mm) and *n*-hexane/ethanol, 86:14 v/v, + water, 0.2% v/v, as mobile phase (flow 1 mL/min, UV detector at 210 nm, injection of 4 μL). All reactions were carried out under anhydrous nitrogen atmosphere using standard Schlenk techniques. Most chemicals and solvents were analytical grade and used without further purification.

2-(4-Fluoro-2-methylphenyl)pyrazine (3). To a solution of 2-bromo-5-fluorotoluene (1.36 g, 3.28 mmol) in toluene (20 mL), EtOH 95% (10 mL) and 1 M solution of Na_2CO_3, (20 mL) were added followed by [1,2-[bis(diphenylphosphino)ethane]dichloronickel(II) (0.21 g, 0.23 mmol) and chloropyrazine (1 mL, 11.17 mmol). The reaction mixture was refluxed for 2 h and then poured into AcOEt (100 mL). The organic layer was extracted with brine (4 × 25 mL), dried over Na_2SO_4, and evaporated in vacuo. The crude residue was purified by flash chromatography (cyclohexane/AcOEt, 8:2) to give the title compound as white solid (1.4 g, 76%). Mp 66−68 °C. ^{1}H NMR (400 MHz, DMSO-d_6): δ (ppm) 8.81 (d, 1H), 8.72 (m, 1H), 8.63 (d, 1H), 7.52 (m, 1H), 7.22 (m, 1H), 7.17 (m, 1H), 2.35 (s, 3H). MS: *m*/*z* 189.

2-(4-Fluoro-2-methylphenyl)piperazine (4). To a solution of compound **3** (0.3 g, 1.59 mmol) in EtOH, 95% (20 mL), were added HCl 37% (0.2 mL) and $Pd(OH)_2$/C 20% (30 mg). The reaction mixture was hydrogenated at 5 atm at room temperature for 4 h, then filtered and concentrated in vacuo. The solid residue was washed with a mixture of AcOEt/AcOH, 2:1 (30 mL), then with small portions of cold AcOEt, dried overnight at 50 °C in vacuo to give **4** (320 mg, 70%). Mp >220 °C. ^{1}H NMR (400 MHz, DMSO-d_6): δ (ppm) 9.72 (bs, 2H), 7.90 (d, 1H), 7.21−7.17 (m, 2H), 4.85 (m, 1H), 3.57−3.20 (m, 6H), 2.40 (s, 3H). MS: *m*/*z* 195.

Phenylmethyl 3-(4-Fluoro-2-methylphenyl)-1-piperazinecarboxylate (5). Compound **4** (0.25 g, 0.94 mmol) was dissolved under a nitrogen atmosphere in dry CH_2Cl_2 (25 mL). Triethylamine (0.5 mL, 3.77 mmol) was added at 0 °C. Then benzylchloroformate (0.15 mL, 1.05 mmol) was dissolved in dry CH_2Cl_2 (10 mL) and slowly added to the reaction mixture, then stirred at 0 °C for additional 2 h. Brine was added (10 mL), and the organic layer was separated and washed again with brine (2 × 10 mL) and dried over Na_2SO_4. The solvent was evaporated in vacuo and the crude residue was purified by flash chromatography (cyclohexane/AcOEt, 1:1) to give **5** (0.208 g, 68%) as a colorless oil. ^{1}H NMR (400 MHz, $CDCl_3$): δ (ppm) 7.52 (m, 1H), 7.40−7.30 (m, 5H), 6.90−6.80 (m, 2H),

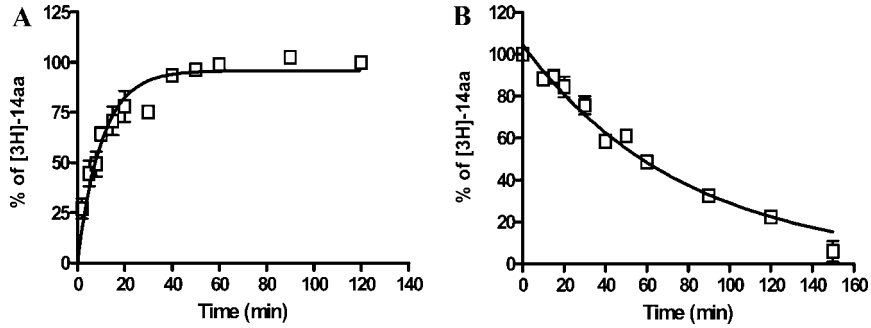

Figure 7. The 0.2nM [^{3}H]**14aa** association (A) and dissociation (B) on membranes from h-NK$_1$ CHO cells. Curves depicted represent the mean fit of three independent experiments performed in duplicate.

5.16 (dd, 2H), 4.12 (m, 2H), 3.86 (m, 1H), 3.30−2.70 (m, 4H), 2.33 (bs, 3H). MS: *m*/*z* 329.

Phenylmethyl-4-{[{[3,5-bis(trifluoromethyl)phenyl]methyl}(methyl)amino]carbonyl}-3-(4-fluoro-2-methylphenyl)-1-piperazinecarboxylate (6). Compound **5** (0.26 g, 0.6 mmol) was dissolved in dry CH_2Cl_2 (35 mL) under a nitrogen atmosphere. Triethylamine (0.32 mL, 2.3 mmol) was added at 0 °C, followed by triphosgene (65 mg, 0.21 mmol) dissolved in CH_2Cl_2 (25 mL). The reaction mixture was stirred at room temperature for 3 h. Then pyridine (0.3 mL, 0.29 mmol) and *N*-methyl-3,5-bis(trifluoromethyl)benzylamine hydrochloride (0.25 g, 0.61 mmol) were added in sequence and the solution was stirred overnight at room temperature. HCl, 1 N (10 mL), was added and the organic layer was separated, washed with brine (3 × 10 mL), dried over Na_2SO_4, and concentrated in vacuo. The crude residue was purified by flash chromatography (cyclohexane/AcOEt, 1:1) to give **6** (85 mg, 36%) as a pale-yellow foam. ^{1}H NMR (400 MHz, $CDCl_3$): δ (ppm) 7.76 (s, 1H), 7.49 (s, 2H), 7.40−7.30 (m, 5H), 7.20 (dd, 1H), 6.86 (d, 1H), 6.79 (m, 1H) 5.17 (s, 2H), 4.66 (d, 1H), 4.64 (m, 1H), 4.36 (d, 1H), 3.97 (m, 2H), 3.4 (m, 2H), 3.16 (m, 2H), 2.93 (s, 3H), 2.38 (bs, 3H). MS: *m*/*z* 612.

***N*-{[3,5-Bis(trifluoromethyl)phenyl]methyl}-2-(4-fluoro-2-methylphenyl)-*N*-methyl-1-piperazinecarboxamide Hydrochloride (7).** Compound **6** (50 mg, 0.08 mmol) was dissolved in EtOH, 95% (10 mL), and hydrogenated (Pd/C, 5%) at 1 atm for 3 h. The catalyst was filtered, and a solution of HCl, 1 M in Et_2O (0.5 mL), was added. The white precipitate was filtered, washed with Et_2O, and dried in vacuo overnight to give the title compound **7** (20 mg). Mp >220 °C. ^{1}H NMR (400 MHz, DMSO-d_6): δ (ppm) 9.33 (bs, 1H), 9.18 (bs, 1H), 7.96 (s, 1H), 7.59 (s, 2H), 7.33 (dd, 1H), 6.99 (d, 1H), 6.85 (t, 2H), 4.66 (d, 1H), 4.53 (dd, 1H), 4.37 (d, 1H), 3.52 (d, 1H), 3.40−3.20 (m, 4H), 2.93 (s, 3H), 2.90 (m, 1H), 2.38 (s, 3H). MS: *m*/*z* 478. IR (Nujol) 3200, 1659 cm^{-1}. MS: *m*/*z* 478.

(1*R*)-1-Phenylethyl 3-(4-fluoro-2-methylphenyl)-1-piperazinecarboxylate (8a,b). To a solution of CDI (162 mg, 1 mmol) in CH_2Cl_2 (5 mL) was added (*R*)-(+)-1-phenethyl alcohol (123 mg, 1 mmol) at room temperature, and reaction mixture was stirred for 30 min. Then compound **4** (180 mg, 0.9 mmol) dissolved in CH_3CN (15 mL) was added and the reaction mixture was refluxed for 24 h. AcOEt (30 mL) and HCl, 1 N (10 mL), were added. The organic layer was separated, washed with brine (3 × 10 mL), dried over Na_2SO_4, and concentrated in vacuo. The crude residue was purified by flash chromatography (cyclohexane/AcOEt, 4:1) to give a mixture of compounds **8a** and **8b** (180 mg, 59%) as a colorless foam. ^{1}H NMR (400 MHz, DMSO-d_6): δ (ppm) 7.87 (m, 1H), 7.40−7.25 (m, 5H), 7.02−6.94 (m, 2H), 5.74 (m, 1H), 3.93−3.71 (m, 3H), 3.00−2.55 (m, 4H), 2.34 (s, 3H), 2.28 (s, 3H). MS: *m*/*z* 343.

(1*R*)-1-Phenylethyl-(3*S*)-4-{[{[3,5-bis(trifluoromethyl)phenyl]-methyl}(methyl)amino]carbonyl}-3-(4-fluoro-2-methylphenyl)-1-piperazinecarboxylate (9a) and (1*R*)-1-Phenylethyl-(3*R*)-4-{[{[3,5-bis-(trifluoromethyl)phenyl]methyl}(methyl)amino]carbonyl}-3-(4-fluoro-2-methylphenyl)-1-piperazinecarboxylate (9b). To a solution of compounds **8a**,**b** (180 mg, 0.55 mmol) dissolved in CH_2Cl_2 (5 mL), triethylamine (0.35 mL, 2.5 mmol) was added at 0 °C. Then a solution of triphosgene (75 mg, 0.25 mmol) dissolved in CH_2Cl_2 (2 mL) was dropped into the reaction mixture. After 2 h, a solution of *N*-methyl-3,5-bis(trifluoromethyl)benzylamine hydrochloride (201 mg, 0.69 mmol) in CH_2Cl_2 (3 mL) was added dropwise and the reaction mixture stirred 4 h at room temperature. CH_2Cl_2 (20 mL) and HCl, 1 N (10 mL), were added. The organic layer was separated, washed with brine (3 × 10 mL), dried over Na_2SO_4, and concentrated in vacuo. The crude residue was purified by flash chromatography (cyclohexane/AcOEt, 7:3) to give pure separated compounds **9a** and **9b** (125 and 135 mg, respectively) and some mixed fractions (45 mg) in 89% total yield.

9a. ^{1}H NMR (400 MHz, DMSO-d_6): δ (ppm) 7.90 (s, 1H), 7.67 (s, 2H), 7.40−7.27 (m, 6H), 6.95 (dd, 1H), 6.80 (m, 1H), 5.74 (q, 1H), 4.60−4.40 (dd, 2H), 4.50 (m, 1H), 3.79 (m, 3H), 3.00 (m, 3H), 2.87 (s, 3H), 2.29 (s, 3H), 1.46 (d, 3H). MS: *m*/*z* 626.

9b. ^{1}H NMR (400 MHz, DMSO-d_6): δ (ppm) 7.90 (s, 1H), 7.67 (s, 2H), 7.37−7.24 (m, 6H), 6.95 (dd, 1H), 6.81 (m, 1H), 5.75 (q, 1H), 4.60−4.41 (dd, 2H), 4.52 (m, 1H), 3.83−3.00 (m, 6H), 2.88 (s, 3H), 2.33 (s, 3H), 1.48 (d, 3H). MS: *m*/*z* 626.

(2*S*)-*N*-{[3,5-Bis(trifluoromethyl)phenyl]methyl}-2-(4-fluoro-2-methylphenyl)-*N*-methyl-1-piperazinecarboxamide Hydrochloride (7a). Compound **9a** (120 mg, 0.2 mmol) was dissolved in EtOH 95% (10 mL) and hydrogenated (Pd/C 5%) at 1 atm for 4 h. The catalyst was filtered and a solution of HCl, 1 M in Et_2O (0.5 mL), was added. The white precipitate was filtered, washed with Et_2O, and dried in vacuo overnight to give the title compound **7a** (57 mg, 55%). Mp >220 °C. ^{1}H NMR (400 MHz, DMSO-d_6): δ (ppm) 9.11 (bs, 1H), 8.83 (bs, 1H), 7.96 (s, 1H), 7.59 (s, 2H), 7.34 (dd, 1H), 6.94 (d, 1H), 6.86 (m, 2H), 4.66 (d, 1H), 4.53 (dd, 1H), 4.36 (m, 1H), 3.54 (m, 1H), 3.44−3.10 (m, 4H), 2.93 (s, 3H), 2.90 (m, 1H), 2.38 (s, 3H). MS: *m*/*z* 478.4. Chiral HPLC (condition A): retention time 14.5 min (98.4% a/a). $[\alpha]_D^{20}$ +69.5 (*c* 0.27, $CHCl_3$).

(2*R*)-*N*-{[3,5-Bis(trifluoromethyl)phenyl]methyl}-2-(4-fluoro-2-methylphenyl)-*N*-methyl-1-piperazinecarboxamide (7b) Hydrochloride. Compound **9b** (130 mg, 0.21 mmol) was dissolved in EtOH, 95% (10 mL), and hydrogenated (Pd/C, 5%) at 1 atm for 4 h. The catalyst was filtered, and a solution of HCl, 1 M in Et_2O (0.5 mL), was added. The white precipitate was filtered, washed with Et_2O, and dried in vacuo overnight to give the title compound **7b** (63 mg, 61%). Mp >220 °C. ^{1}H NMR (400 MHz, DMSO-d_6): δ (ppm) 9.11 (bs, 1H), 8.83 (bs, 1H), 7.96 (s, 1H), 7.59 (s, 2H), 7.34 (dd, 1H), 6.94 (d, 1H), 6.86 (m, 2H), 4.66 (d, 1H), 4.65−4.35 (m, 2H), 3.54 (m, 1H), 3.44−3.10 (m, 4H), 2.93 (s, 3H), 2.90 (m, 1H), 2.38 (s, 3H). MS: *m*/*z* 478. Chiral HPLC (condition A) retention time 15.2 min (98.4% a/a). $[\alpha]_D^{20}$ −72.6 (*c* 0.27, $CHCl_3$).

(4-Fluoro-2-methylphenyl)oxoacetic Acid Methyl Ester (10). To a suspension of magnesium turnings (6.17 g, 253.8 mmol) in dry THF (60 mL) at 20 °C under a nitrogen atmosphere, a small amount of iodine was added, followed by a solution of commercial 2-bromo-5-fluorotoluene **2** (40 g, 211.6 mmol) in dry THF (150 mL). The suspension was gently heated until the brown color disappeared. The remaining bromide solution was added dropwise, maintaining the reaction mixture at 50−60 °C. Then the suspension was stirred at 70 °C for 2 h until the magnesium turnings disappeared. A solution of LiBr

(44.1 g, 507.7 mmol) in 500 mL of anhydrous THF was added dropwise to a suspension of Cu_2Br_2 (36.4 g, 253.8 mmol) in 500 mL of anhydrous THF. The reaction mixture was stirred at 20 °C for 1 h (dark-green solution with a small amount of white solid in suspension). The Grignard reagent solution previously prepared was then added dropwise, maintaining the temperature below 25 °C, followed by methyloxalyl chloride (19.5 mL, 212.0 mmol). The reaction mixture was stirred at 20 °C for 2 h. Then the solvent was evaporated in vacuo and the residue was taken up in AcOEt (1500 mL). The organic layer was washed with saturated aqueous NH_4Cl (2 × 1000 mL) and dried over anhydrous Na_2SO_4, filtered, evaporated in vacuo; the crude oil was purified by flash chromatography (cyclohexane/AcOEt, 95:5) to give the title compound as an oil (24.4 g, 58.5%). ^{1}H NMR (400 MHz, $CDCl_3$): δ (ppm) 7.74 (m, 1H), 6.98−7.04 (m, 2H), 3.96 (s, 3H), 2.61 (s, 3H). MS: *m*/*z* 197.

3-(4-Fluoro-2-methylphenyl)-5,6-dihydro-1*H*-pyrazin-2-one (11). To a solution of intermediate **10** (20.1 g, 101.8 mmol) and ethylenediamine (6.8 mL, 101.8 mmol) in 400 mL of toluene, anhydrous Na_2SO_4 (20 g) was added at 20 °C under nitrogen atmosphere. The reaction mixture was heated at reflux for 6 h. Then the reaction mixture was cooled and filtered. The solvent was evaporated in vacuo and the crude oil was purified by flash chromatography (AcOEt), affording the title compound as a white solid (12.9 g, 61.4%). ^{1}H NMR (400 MHz, $CDCl_3$): δ (ppm) 7.33 (m, 1H), 6.95−6.90 (m, 2H), 6.56 (m, 1H), 3.97 (m, 2H), 3.58 (m, 2H), 2.31 (s, 3H). MS: *m*/*z* 207.

3-(4-Fluoro-2-methylphenyl)piperazin-2-one (12). To a solution of intermediate **11** (11.76 g, 57.0 mmol) in CH_3OH (170 mL), Pd/C, 10% (3 g), was added, and the reaction mixture was hydrogenated at 1 atm at room temperature for 16 h. Then the catalyst was filtered and the solvent was evaporated to low volume (30 mL). CH_3OH (140 mL) and AcOEt (700 mL) were added, and the solution was rapidly filtered by a silica pad (60 g). The eluted solution was evaporated in vacuo to obtain the title compound (11.76 g, 99.0%). ^{1}H NMR (400 MHz, DMSO-d_6): δ (ppm) 7.77 (bm, 1H), 7.24 (dd, 1H), 6.96 (dd, 1H), 6.92 (td, 1H), 4.43 (s, 1H), 3.30 (m, 1H), 3.14 (m, 1H), 2.92 (m, 1H), 2.82 (m, 2H), 2.33 (s, 3H). MS: *m*/*z* 209.

(+)-(*S*)-3-(4-Fluoro-2-methylphenyl)piperazin-2-one (12a). To a suspension of racemic intermediate **12** (5.25 g, 25.2 mmol) in 135 mL of AcOEt, *S*-(+)-mandelic acid (4.095 g, 26.9 mmol) was added. The suspension was stirred at room temperature for 1 h and then at 3−5 °C for an additional 2 h, filtered, and evaporated in vacuo to give crude L-(+)mandelate 3-(4-fluoro-2-methylphenyl)piperaz- in-2-one **12a**, which was suspended in AcOEt (55 mL). The solution was refluxed until complete dissolution occurred, then cooled to room temperature and stirred for 2 h, filtered, and dried in vacuo to obtain a white solid. This material was suspended in AcOEt (45 mL), and an amount of 22 mL of a 0.73 M solution of NaOH, saturated with NaCl, was added. The organic layer was separated and washed with H_2O (15 mL). Then the aqueous layer was extracted with AcOEt (4 × 15 mL). The combined organic layers were dried over anhydrous Na_2SO_4 and concentrated in vacuo to give the title compound (2.17 g, 41.3%) as a white foam. ^{1}H NMR (400 MHz, DMSO-d_6): δ (ppm) 7.77 (bm, 1H), 7.24 (dd, 1H), 6.96 (dd, 1H), 6.92 (td, 1H), 4.43 (s, 1H), 3.30 (m, 1H), 3.14 (m, 1H), 2.92 (m, 1H), 2.82 (m, 2H), 2.33 (s, 3H). Chiral HPLC (condition A) retention time 7.9 min (98.2% a/a). $[\alpha]_D^{20}$ +17.9 (*c* 1.17, $CHCl_3$). MS: *m*/*z* 209.

(−)-(*R*)-3-(4-Fluoro-2-methylphenyl)piperazin-2-one (12b). To a suspension of racemic intermediate **12** (5.25 g, 25.2 mmol) in AcOEt (135 mL), *R*-(−)-mandelic acid (4.095 g, 26.9 mmol) was added. The suspension was stirred at room temperature for 1 h and then at 3−5 °C for 2 h, filtered, and dried in vacuo to obtain crude *R*-(−)mandelate 3-(4-fluoro-2-methylphenyl)piperazin-2-one (5.55 g), which was suspended in AcOEt (55.5 mL) and heated to reflux until complete dissolution. Then the solution was cooled to room temperature and stirred for 2 h, filtered, washed with AcOEt (22 mL), and dried in vacuo to give a white solid. This material was suspended in AcOEt (45 mL), and an amount of 22 mL of a 0.73 M solution of NaOH, saturated with NaCl, was added. The organic layer was separated and washed with H_2O (15 mL). The aqueous layer was extracted with AcOEt (4 × 15 mL). The combined organic phases were dried over Na_2SO_4 and concentrated in vacuo to give the title compound (2.17 g, 41.3%) as a white foam. ^{1}H NMR (400 MHz, DMSO-d_6): δ (ppm) 7.79 (bm, 1H), 7.23 (dd, 1H), 6.97 (dd, 1H), 6.91 (td, 1H), 4.45 (s, 1H), 3.31 (m, 1H), 3.14 (m, 1H), 2.93 (m, 1H), 2.84 (m, 2H), 2.32 (s, 3H). Chiral HPLC (condition A): retention time 7.2 min (98.1% a/a). $[\alpha]_D^{20}$ −18 (*c* 1.17, $CHCl_3$). MS: *m*/*z* 209.

2-(*S*)-(4-Fluoro-2-methylphenyl)-3-oxopiperazine-1-carboxylic Acid [1-(*R*)-(3,5-Bis-trifluoromethylphenyl)ethyl]methylamide (13aa) and 2(*S*)-(4-Fluoro-2-methylphenyl)-3-oxopiperazine-1-carboxylic Acid [1-(*S*)-(3,5-Bis-trifluoromethylphenyl)ethyl]methylamide (13ab). To a solution of intermediate **12a** (1.21 g, 5.8 mmol) in 27 mL of dry CH_2Cl_2, Et_3N (1.64 mL, 11.8 mmol) was added. The solution was cooled to 0 °C, and a solution of triphosgene (0.73 g, 2.46 mmol) in dry CH_2Cl_2 (6 mL) was dropped into the reaction mixture in 40 min. The solution was stirred 4 h at 0 °C and then brought back to room temperature. Diisopropylethylamine (2 mL, 11.5 mmol) was added, followed by a solution of 1-[3,5-bis(trifluoromethyl)phenyl]ethyl]-*N*-methylamine (2.36 g, 8.7 mmol) dissolved in 60 mL of CH_3CN in acetonitrile. After evaporation of the CH_2Cl_2, the internal temperature was brought to 70 °C and the reaction flask was equipped with a water condenser, and the mixture was stirred for 2 h. Then the solvent was evaporated in vacuo and the residue was partitioned between CH_2Cl_2 and HCl, 1 M, and the separated organic layer was dried over anhydrous Na_2SO_4, filtered, and evaporated in vacuo to give a crude residue which was purified by flash chromatography (AcOEt/cyclohexane, 8:2) to afford the title compounds **13aa** (0.88 g, 1.74mmol, 30.0%) and **13ab** (0.89 g, 30.3%) as white foams.

13aa. ^{1}H NMR (500 MHz, DMSO-d_6): δ 8.16 (s. 1H), 7.98 (s, 2H), 7.71 (bs, 2H), 7.19 (dd, 1H), 6.97 (dd, 1H), 6.87 (td, 1H), 5.34 (s, 1H), 5.14 (q, 1H), 3.45−3.2 (m, 4H), 2.53 (s, 3H), 2.27 (s, 3H), 1.56 (d, 3H). MS: *m*/*z* 506.

13ab. ^{1}H NMR (500 MHz, DMSO-d_6): δ 8.16 (s, 1H), 7.95 (s, 2H), 7.70 (bs, 2H), 7.19 (dd, 1H), 6.98 (dd, 1H), 6.90 (td, 1H), 5.29 (q, 1H), 5.28 (s, 1H), 3.45−3.15 (m, 4H), 2.66 (s, 3H), 2.27 (s, 3H), 1.52 (d, 3H). MS: *m*/*z* 506.

2-(*R*)-(4-Fluoro-2-methylphenyl)-3-oxopiperazine-1-carboxylic Acid [1-(*R*)-(3,5-Bis-trifluoromethylphenyl)ethyl]-methylamide (13ba) and 2(*R*)-(4-Fluoro-2-methylphenyl)-3-oxopiperazine-1-carboxylic Acid [1-(*S*)-(3,5-Bis-trifluoromethylphenyl)ethyl]methylamide (13bb). To a solution of intermediate **12b** (1.2 g, 5.76 mmol) in dry CH_2Cl_2 (27 mL), Et_3N (1.64 mL, 11.8 mmol) was added. The solution was cooled to 0 °C, and a solution of triphosgene (0.72 g, 2.43 mmol) in dry CH_2Cl_2 (6 mL) was added dropwise over 40 min. The reaction mixture was stirred at 0 °C for 4 h, then was brought back to room temperature. Diisopropyltriethylamine (2 mL, 11.5 mmol) was then added, followed by a solution of 1-[3,5-bis(trifluoromethyl)phenyl]ethyl]-*N*-methylamine (2.35 g, 8.66 mmol) in CH_3CN (60 mL). After evaporation of the CH_2Cl_2, the mixture was heated at 70 °C for an additional 2 h. The solvent was evaporated in vacuo, and the residue was partitioned between CH_2Cl_2 and HCl, 1M. The aqueous layer was extracted with CH_2Cl_2, and the combined organic extracts were dried over anhydrous Na_2SO_4, filtered, and evaporated in vacuo to give a crude residue which was purified by flash chromatography (AcOEt/cyclohexanes, 8:2) to obtain the title compounds **13ba** (0.88 g, 1.74 mmol, 30%) and **13bb** (0.9 g, 30.7%) as white foams.

13ba. ^{1}H NMR (500 MHz, DMSO-d_6): δ 8.15 (s, 1H), 7.97 (s, 2H), 7.71 (bs, 2H), 7.18 (dd, 1H), 6.97 (dd, 1H), 6.85 (td, 1H), 5.33 (s, 1H), 5.14 (q, 1H), 3.45−3.2 (m, 4H), 2.52 (s, 3H), 2.26 (s, 3H), 1.55 (d, 3H). MS: *m*/*z* 506.

13bb. ^{1}H NMR (500 MHz, DMSO-d_6): δ 8.15 (s, 1H), 7.95 (s, 2H), 7.70 (bs, 2H), 7.19 (dd, 1H), 6.99 (dd, 1H), 6.89 (td, 1H), 5.29 (q, 1H), 5.28 (s, 1H), 3.45−3.15 (m, 4H), 2.66 (s, 3H), 2.27 (s, 3H), 1.52 (d, 3H). MS: *m*/*z* 506.

2-(*S*)-(4-Fluoro-2-methylphenyl)piperazine-1-carboxylic Acid [1-(*R*)-(3,5-Bis-trifluoromethylphenyl)ethyl]methylamide Acetate Salt (14aa), 2-(*S*)-4-Fluoro-2-methylphenyl)piperazine-1-carboxylic Acid [1-(*S*)-(3,5-Bis-trifluoromethylphenyl)ethyl]-methylamide Acetate Salt (14ab), 2-(*R*)-(4-Fluoro-2-methyl-phenyl)piperazine-1-carboxylic Acid [1-(*S*)-(3,5-Bis-trifluoromethyl-phenyl)ethyl]methyl-amide Acetate Salt (14bb), and 2-(*R*)-4-Fluoro-2-methylphenyl)piperazine-1-carboxylic Acid [1-(*R*)-(3,5-Bis-trifluoromethylphenyl)ethyl]methylamide Acetate Salt (14ba). To a solution of pure intermediate **13aa**, **13ab**, **13ba**, or **13bb** (0.76 g 1.5 mmol) in dry THF (10 mL) was added under nitrogen atmosphere 1 M BH_3·THF solution in THF (8 mL, 8 mmol), and the reaction mixture was refluxed for 3 h. Then an amount of 2.5 mL of HCl, 12 N, was added at 0 °C and the solution was stirred at room temperature for 45 min. Then 6.5 mL of H_2O was added along with 3.2 g of $NaHCO_3$ until neutral pH was attained. The solvent was evaporated, and the aqueous phase was extracted with Et_2O (3 × 10 mL). The combined organic layers were washed with saturated $NaHCO_3$ (10 mL), brine, dried over anhydrous Na_2SO_4, and evaporated in vacuo to give **14aa**, **14ab**, **14ba**, or **14bb**, respectively (0.660, 0.42, 0.18, and 0.19 g), as colorless oils

Theses materials were dissolved in Et_2O (8 mL), and acetic acid (0.07 mL) was added dropwise. The mixture was stirred at 20 °C for 2 h and then at 0 °C for 2 h. The suspensions were filtered and dried in vacuo to give the title compounds (0.26 g and 31.4%, 0.17 g and 31.1%, 0.128 g and 34.5%, 0.069 g and 21.8%, respectively) as a white solids.

14aa. ^{1}H NMR (500 MHz, DMSO-d_6): δ (ppm) 7.99 (s, 1H), 7.71 (s, 2H), 7.28 (m, 1H), 6.92 (m, 1H), 6.77 (m, 1H), 5.28 (q, J = 6.5 Hz, 1H), 4.22 (dd, J = 11.7, 3.4 Hz, 1H), 3.3−2.7 (m, 6H), 2.69 (s, 3H), 2.32 (s, 3H), 1.90 (s, 3H), 1.48 (d, J = 6.9 Hz, 3H); ^{19}F-NMR (300 MHz, DMSO-d_6): δ (ppm) −61.6 (m), −116.3 (s). MS: m/z 492 [M − CH_3COO]$^+$, 341 [$C_{14}H_{15}F_6N_2O$]$^+$, 221 [$C_{12}H_{14}FN_2O$]$^+$. Chiral HPLC (condition B): retention time 4.56 min (98.5% a/a). $[\alpha]_D^{20}$ −120.4 (c 1, $CHCl_3$).

14ab. ^{1}H NMR (400 MHz, DMSO-d_6): δ (ppm) 7.93 (s, 1H), 7.59 (s, 1H), 7.29 (m, 1H), 6.90 (m, 1H), 6.77 (m, 1H), 5.33 (q, 1H), 4.19 (m, 1H), 3.2−2.6 (m, 6H), 2.80 (s, 3H), 2.32 (s, 3H), 1.89 (s, 3H), 1.49 (d, 3H). MS (m/z): 492 [M − CH_3COO]$^+$. Chiral HPLC (condition B): retention time 14.28 min (97% a/a). $[\alpha]_D^{20}$ −164.9 (c 1, $CHCl_3$)

14ba. ^{1}H NMR (400 MHz, DMSO-d_6): δ (ppm) 7.92 (bs, 1H), 7.58 (bs, 1H), 7.28 (m, 1H), 6.89 (m, 1H), 6.76 (m, 1H), 5.32 (q, 1H), 4.18 (dd, 1H), 3.23 (m, 1H), 2.90−2.65 (m, 5H), 2.79 (s, 3H), 2.31 (s, 3H), 1.88 (s, 3H), 1.47 (d, 3H). MS: m/z 492 [M − CH_3COO]$^+$. Chiral HPLC (condition B): retention time 5.20 min (97.8% a/a). $[\alpha]_D^{20}$ +2.2 (c 1.17, $CHCl_3$).

14bb. ^{1}H NMR (500 MHz, DMSO-d_6): δ (ppm) 7.98 (s, 1H), 7.71 (s, 2H), 7.26 (m, 1H), 6.90 (m, 1H), 6.76 (m, 1H), 5.27 (q, 1H), 4.21 (dd, 1H), 3.2−2.6 (m, 6H), 2.68 (s. 3H), 2.3 (s, 3H), 1.88 (s, 3H), 1.47 (d, 3H). MS: m/z 492 [M − CH_3COO]$^+$. Chiral HPLC (condition B): retention time 4.15 min (98.1% a/a). $[\alpha]_D^{20}$ +207 (c 1, $CHCl_3$).

In Vitro and in Vivo Biological Characterization. Materials. [^{3}H]SP (1.26 TBq/mmol) was purchased from Amersham Life Science. **14aa** acetate salt, labeled with [^{3}H] by Amersham Life Science, has been provided as a 3.11 TBq/mmol, ethanol solution. GR205171 was synthesized in house. L-733,060, hydrochloride, was purchased from RBI. SP and GR73632 (δ-aminovaleryl^6, Pro^9, *N*-Me-Leu^{10})substance P (6−11) were obtained from Bachem. All drugs were prepared as 10 mM solution. In binding experiments vs [^{3}H]SP, all competing drugs were serially diluted in the assay buffer. In [^{3}H]**14aa** binding experiments and FLIPR assays, drugs were serially diluted in DMSO to have a final concentration of the solvent equal to 1%. Fluo-4 was purchased from Molecular Probes. Probenecid was purchased from Aldrich.

In Vitro NK_1 Receptor Binding Experiments. Membranes from Chinese hamster ovary cells stably transfected with human NK_1 receptor (h-NK_1 CHO) were prepared essentially as described by Beattie et al. (1995).[23] [^{3}H]SP and [^{3}H]**14aa** binding assays were carried out in 96-well plates in a final volume of 400 μL of 50 mM HEPES, pH 7.4, 3 mM $MnCl_2$, and 0.02% BSA. In [^{3}H]**14aa** binding experiments, 1% DMSO was included in the assay. Incubations proceeded at 22 °C ([^{3}H]SP) or 37 °C ([^{3}H]**14aa**) for 60 min. Displacement experiments were performed by using 0.5 nM [^{3}H]SP. Nonspecific binding was defined by the addition of 1 μM GR205171. Reactions were stopped by filtration through GF/C filtermats using a cell harvester. Association of [^{3}H]**14aa** to h-NK_1 receptors was studied by incubating the membranes with 0.2 nM radioligand for increasing times (from 2 to 120 min). In dissociation experiments, membranes were incubated with 0.2 nM [^{3}H]**14aa** for 60 min; separation of [^{3}H]**14aa** from the receptor was then obtained by blocking the reassociation of the radioligand at different times (from 2 to 180 min) through the addition of 100 nM cold **14aa**.

In Vitro NK_1 Receptor Functional Studies. In functional experiments, the ability of **14aa** to inhibit SP-induced release of $[Ca^{2+}]_i$ in h-NK_1 CHO cells was evaluated. After 30 min of labeling with the cytoplasmic calcium indicator Fluo-4 AM (2 μM), h-NK_1 CHO cells were washed and incubated in the absence or presence of antagonists for 60 min at 37 °C in Hank's balanced salts with 20 mM HEPES and 2.5 mM probenecid, and then concentration−response curves of SP (nM) were performed. Fluorescence was monitored using a FLIPR (λ_{EX} = 488 nm, λ_{EM} = 510−570 nm).

Inhibition of GR73632-Induced Foot Tapping in Gerbils. A well validated procedure to explore the central inhibitory activity of selective NK_1 receptor antagonists was applied to characterize the in vivo activity of the tested compounds.[25] A characteristic intense foot tapping behavior was invoked in male mongolian gerbils (45−70 g, Charles River Italy) by intracerebroventricular (icv) infusion of a highly selective tachykinin NK_1 receptor agonist, GR73632, in gerbils evoking a vigorous species-specific behavior. This rhythmic hind limb thumping is not induced by agonist for the other tachykinin receptors. The skull was exposed, and an amount of 5 μL [3 pmol/5 μL of GR73632] was injected by the insertion of a cuffed 25 gauge needle to a depth of 4 mm below bregma, directly into the lateral ventricle. The scalp incision was closed. The animal was allowed to recover from anesthesia and was individually placed in a clear Perspex observation box (25 cm × 20 cm × 20 cm). Following a minute of recovery, the duration of repetitive hind foot tapping was recorded for 3 min, giving a maximum possible duration of 180 s.

The ability of different compounds to inhibit GR73632-induced foot tapping following oral administration is included here for the purpose of comparison. At 1, 4, 8, or 24 h before the GR73632 administration, at least seven animals each received treatment of vehicle or test compound (10 mL/kg).

Data Analysiss. Receptor Binding and Functional Studies. Radioligand binding data were analyzed by nonlinear regression analysis using GraphPad Prism 4.0 (GraphPad Software, CA). Determination of K_D and B_{max} of radioligands was assessed by elaborating saturation experiments using one site binding (hyperbola) equation. Curve fitting from competition binding experiments was determined by using one site competition equation after checking, with the F test ($P < 0.05$), that the Hill slope in the four-parameter logistic equation was not statistically different from 1.0. In this condition, IC_{50} values were converted to K_i using the Cheng−Prusoff equation.[26] Results are expressed as the mean pK_i ± SEM. [^{3}H]**14aa** kinetic association and dissociation expriments were elaborated with GraphPad Prism by using one phase exponential association and one phase exponential decay, respectively. The ratio of kinetic parameters K_{off}/K_{on} was used to estimate the pK_D value of [^{3}H]**14aa**.

In functional studies, SP concentration−response curves in the presence or absence of fixed concentrations of test drugs where fitted using a four-parameter logistic equation in GraphPad Prism. The potency (pK_B) of compound **1** was determined by using Schild analysis.[27] The apparent pK_B value of **14aa** was estimated by using the Gaddum equation: $pK_B = \log(DR - 1) - \log[A]$, where DR is the ratio of equiactive agonist concentrations in the presence and absence of a fixed antagonist concentration [A].

Combined dose ratio analysis to investigate the competitive or noncompetitive nature of **14aa** antagonism was performed according to the procedure developed by Shankley et al.[21] In brief, the theory

predicts that when two antagonists (A and C) act through a syntopic interaction at the receptor (additive model), then the measured dose ratio in the presence of both the antagonists should be $DR_{A+C} = DR_A + DR_C - 1$, where DR_A and DR_C are the dose ratios obtained independently in the presence of the antagonists A and C. On the contrary, when the two antagonists act independently through an allotropic action (multiplicative model), the measured dose ratio should be $DR_{AC} = DR_A DR_C$.

Data from gerbil foot tapping studies were subjected to one-way analysis of variance (ANOVA) followed by Dunnet's *t* test, using GB-stat software (version 6.5, Dynamic Microsystems Inc.). The doses of compounds inhibiting foot tapping by 50% (ID_{50}) were determined by a linear regression analysis using RS-1 software (±95% CI).

Data of number of postures or jumps reduction were subjected to a paired *t* test using GB-stat software, comparing each compound dose with the related vehicle treatment in the four designed Latin squares.

Supporting Information Available: HPLC chromatograms of compounds **7a**, **7b**, **14aa**, **14ab**, **14ba**, **14bb**. This material is available free of charge via the Internet at http://pubs.acs.org.

References

(1) Chahl, L. A. Tackykinins and neuropsychiatric disorders. *Curr. Drug Targets* **2006**, *7*, 993–103.

(2) Ebner, K.; Singewald, N. The role of substance P in stress and anxiety responses. *Amino Acids* **2006**, *31*, 251–272.

(3) McLean, S. Do substance P and NK_1 receptor have a role in depression and anxiety? *Curr. Pharm. Des.* **2005**, *11*, 1529–1547.

(4) Nemeroff, C. B. Recent advances in the neurobiology of depression. *Psychopharmacol. Bull.* **2002**, *36*, 6–23.

(5) Mantyh, P. W. Neurobiology of substance P and NK_1 receptor. *J. Clin. Psychiatry* **2002**, *63*, 6–10.

(6) Wong, M. L.; Licinio, J. From monoamine to genomic targets: a paradigm shift for drug discovery in depression. *Nat. Rev. Drug Discovery* **2004**, *3*, 136–151.

(7) Holtzheimer, P. E.; Nemeroff, C. B. Novel targets for antidepressant therapies. *Curr. Psychiatry Rep.* **2008**, *10*, 465–473.

(8) Patacchini, R.; Maggi, C. A. Peripheral tachikinin receptors as targets for new drugs. *Eur. J. Pharmacol.* **2001**, *429*, 13–21.

(9) Rupniak, N. M.; Kramer, M. S. Discovery of the antidepressant and antiemetic efficacy of substance P receptor (NK_1) antagonists. *TIPS* **1999**, *20*, 485–490.

(10) Kramer, M. S.; Cutler, N.; Feighner, J.; Shrivastava, R.; Carman, J.; Sramek, J. J.; Reines, S. A.; Liu, G.; Snavely, D.; Wyatt-Knowles, E.; Hale, J. J.; Mills, S. G.; MacCoss, M.; Swain, C. J.; Harrison, T.; Hill, R. G.; Hefti, F.; Scolnick, E. M.; Cascieri, M. A.; Chicchi, G. G.; Sadowski, S.; Williams, A. R.; Hewson, L.; Smith, D.; Carlson, E. J.; Hargreaves, R. J.; Rupniak, N. M. J. Distinct mechanism for antidepressant activity by blockade of central substance P receptors. *Science* **1998**, *281*, 1640–1645.

(11) Kramer, M. S.; Winokur, A.; Kelsey, J.; Preskorn, S. H.; Rothschild, A. J.; Snavely, D.; Ghosh, K.; Ball, W. A.; Reines, S. A; Munjack, D.; Apter, J. T; Cunningham, L.; Kling, M.; Bari, M.; Getson, A.; Lee, Y. Demonstration of the efficacy and safety of a novel substance P (NK_1) receptor antagonist in major depression. *Neuropsychopharmacology* **2004**, *29*, 385–392.

(12) Chappell, P. Effects of CP122721, a Selective NK_1 Receptor Antagonist in Patients with Major Depression. Presented at the 42nd Annual Meeting of the New Clinical Drug Evaluation Unit (NCDEU), Boca Raton, FL, Jun 12, 2002.

(13) In a phase II trial in 300 social anxiety disorder patients, NKP-608 at 0.1 and 1.0 mg for 8 weeks improved the Liebowitz social anxiety scale of placebo with no adverse events (Company Web Page, Novartis, Jan 16, 2001).

(14) Furmark, T.; Appel, L.; Michelgård, A.; Wahlstedt, K.; Åhs, F.; Zancan, S.; Jacobsson, E.; Flyckt, K.; Grohp, M.; Bergström, M.; Merlo-Pich, E.; Nilsson, L. G.; Bani, M.; Långström, B.; Fredrikson, M. Cerebral blood flow changes after treatment of social phobia with the neurokinin-1 antagonist GR205171, citalopram, or placebo. *Biol. Psychiatry* **2005**, *58*, 132–142.

(15) Ranka, K.; Krishnan, R. Clinical experience with substance P receptor (NK1) antagonists in depression. *J. Clin. Psychiatry* **2002**, *63*, 25–29.

(16) Herpfer, I.; Lieb, K. Substance P receptor antagonists in psychiatry: rationale for development and therapeutic potential. *CNS Drugs* **2005**, *19*, 275–293.

(17) Armour, D. R.; Chung, K. M. L.; Congreve, M.; Evans, B.; Hubbard, T.; Kay, C.; Middlemiss, D.; Mordaunt, J. E.; Pegg, N. A.; Vinader, P.; Ward, P.; Watson, S. P. Tetrazole NK_1 receptor antagonists: the identification of an exceptionally potent orally active antiemetic compound. *Bioorg. Med. Chem. Lett.* **1996**, *6*, 1015–1020.

(18) Griffante, C.; Carletti, R.; Andreetta, F.; Corsi, M. [^{3}H]-GR205171 displays similar NK_1 receptor binding profile in gerbil and human brain. *Br. J. Pharmacol.* **2006**, *148*, 39–45.

(19) Beresford, I. J. M.; Birch, P.J.; Hagan, R. M.; Ireland, S. J. Investigation into species variants in tachykinin NK_1 receptors by use of the non-peptide antagonist CP-96,345. *Br. J. Pharmacol.* **1991**, *104*, 292–293.

(20) A preliminary part of this work was reported at the ECNP meeting (Amsterdam) in 2005: P.4.027, P.4.052, P.4.053.

(21) Shankley, N. P.; Black, J. W.; Ganellin, C. R.; Mitchell, R. C. Correlation between log $P_{OCT/H2O}$ and pK_B estimates for a series of muscarinic and histamine H2-receptor antagonists. *Br. J. Pharmacol.* **1988**, *94*, 264–274.

(22) Seabrook, G. R.; Shepheard, S. L.; Williamson, D. J.; Tyrer, P.; Rigby, M.; Cascieri, M.A; Harrison, T.; Hargreaves, R. J.; Hill, R. G. L-733,060, a novel tachykinin NK_1 receptor antagonist; effects in $[Ca^{2+}]_i$ mobilisation, cardiovascular and dural extravasation assays. *Eur. J. Pharmacol.* **1996**, *317*, 129–135.

(23) Vauquelin, G.; Van Liefde, I. V. Slow antagonist dissociation and long-lasting in vivo receptor protection. *TIPS* **2006**, *27*, 355–359.

(24) Beattie, D. T.; Beresford, I. J.; Connor, H. E.; Marshall, F. H.; Hawcock, A. B.; Hagan, R. M.; Bowers, J.; Birch, P. J.; Ward, P. The pharmacology of GR203040, a novel, potent and selective non-peptide tachykinin NK_1 receptor antagonist. *Br. J. Pharmacol.* **1995**, *116*, 3149–3157.

(25) Rupniak, N. M. J.; Williams, A. R. Differential inhibition of foot tapping and chromodacryorrhoea in gerbils by CNS penetrant and non-penetrant tachykinin NK-1 receptor antagonists. *Eur. J. Pharmacol.* **1994**, *265*, 179–183.

(26) Cheng, Y.; Prusoff, W. H. Relationship between the inhibition constant (K1) and the concentration of inhibitor which causes 50% inhibition (I50) of an enzymatic reaction. *Biochem. Pharmacol.* **1973**, *22*, 3099–3108.

(27) Arunlakshana, O.; Schild, H. O. Some quantitative uses of drug antagonists. *Br. J. Pharmacol.* **1959**, *14*, 48–58.

JM900023B